

# Online Research @ Cardiff

This is an Open Access document downloaded from ORCA, Cardiff University's institutional repository: <https://orca.cardiff.ac.uk/id/eprint/99011/>

This is the author's version of a work that was submitted to / accepted for publication.

Citation for final published version:

De Almeida, Andreia ORCID: <https://orcid.org/0000-0002-6889-1503>, Mosca, Andreia F., Wragg, Darren, Wenzel, Margot ORCID: <https://orcid.org/0000-0001-6411-1816>, Kavanagh, Paul, Barone, Giampaolo, Leoni, Stefano ORCID: <https://orcid.org/0000-0003-4078-1000>, Soveral, Graca and Casini, Angela ORCID: <https://orcid.org/0000-0003-1599-9542> 2017. The mechanism of aquaporin inhibition by gold compounds elucidated by biophysical and computational methods. Chemical Communications 53 (27) , pp. 3830-3833. 10.1039/C7CC00318H file

Publishers page: <http://dx.doi.org/10.1039/C7CC00318H>  
<<http://dx.doi.org/10.1039/C7CC00318H>>

Please note:

Changes made as a result of publishing processes such as copy-editing, formatting and page numbers may not be reflected in this version. For the definitive version of this publication, please refer to the published source. You are advised to consult the publisher's version if you wish to cite this paper.

This version is being made available in accordance with publisher policies.

See

<http://orca.cf.ac.uk/policies.html> for usage policies. Copyright and moral rights for publications made available in ORCA are retained by the copyright holders.



# The mechanism of aquaporin inhibition by gold compounds elucidated by biophysical and computational methods

Andreia de Almeida,<sup>a,\*</sup> Andreia F. Mósca,<sup>b,c,\*</sup> Darren Wragg,<sup>a</sup> Margot Wenzel,<sup>a</sup> Paul Kavanagh,<sup>d</sup> Giampaolo Barone,<sup>e</sup> Stefano Leoni,<sup>a</sup> Graça Soveral,<sup>b,c,\*</sup> Angela Casini<sup>a,\*</sup>

The inhibition of water and glycerol permeation via human aquaglyceroporin-3 (AQP3) by gold(III) complexes has been studied by stopped-flow spectroscopy and, for the first time, its mechanism has been described using molecular dynamics (MD), combined to density functional theory (DFT) and electrochemical studies. The obtained MD results showed that the most effective gold-based inhibitor, anchored to Cys40 in AQP3, is able to induce shrinkage of the pore preventing glycerol and water permeation. Moreover, good correlation between the Au(III) complex affinity to Cys binding and AQP3 inhibition effects was highlighted, while no influence of the different oxidative character of the complexes could be observed.

## Introduction

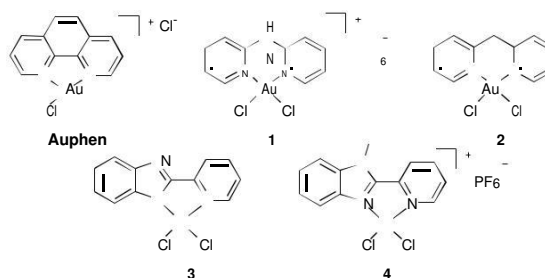
Water cellular movement is a prerequisite for all life forms. In fact, the fundamental discovery and characterization of an abundant protein of the erythrocyte membrane, termed Aquaporin-1 (AQP1), 25 years ago, represented a paradigm shift in the understanding of molecular, membrane and organism water transport. Since then, several studies have shown that AQP1 is a member of a widespread family of water and solute-permeable membrane proteins – *Aquaporins* (AQPs) – which have been demonstrated to be ubiquitous in all domains of life.<sup>1</sup>

In mammals, the 13 aquaporin isoforms identified so far (AQP0-12) expressed in a wide range of tissues, organized as tetramers in membranes, and can permeate water (orthodox aquaporins), glycerol (aquaglyceroporins), and other small solutes.<sup>2</sup> These membrane channels play important roles in physiology and pathophysiology, *e.g.* maintaining cellular homeostasis and being essential in cellular metabolism. Thus, they have been suggested as potential *targets for drug development*.<sup>3-5</sup> Specifically, aquaglyceroporins regulate glycerol content in epidermis, fat and other tissues and appear to be involved in skin hydration, cell proliferation, carcinogenesis and fat metabolism.<sup>1,6</sup>

To validate the various roles of AQPs in health and disease,

and to develop AQP-targeted therapies, in addition to genetic approaches, the use of selective inhibitors holds great promise. However, so far no reported small-molecule AQP inhibitors possess sufficient isoform selectivity to be good candidates for clinical development.<sup>7</sup> In this context, for the first time we reported on the potent and selective inhibition of human aquaglyceroporin-3 (AQP3) by a water-soluble Au(III) compound, [Au(phen)Cl<sub>2</sub>]<sup>+</sup>Cl<sup>-</sup> (phen = 1,10-phenanthroline) (Auphen, Fig. 1).<sup>8</sup> Of note, Auphen inhibited glycerol transport in human red blood cells (hRBC) with an IC<sub>50</sub> = 0.8 ± 0.08 μM, while having no inhibitory effect on AQP1-mediated water permeability. Using *in silico* approaches, we investigated the non-covalent binding of Auphen at a molecular level and found that its isoform selectivity is due to the accessibility of Cys40, whose thiol group is a likely candidate for direct binding to Au(III) complexes.<sup>8</sup> The involvement of this residue in the inhibition mechanism was further confirmed by site-directed mutagenesis studies.<sup>9</sup>

Figure 1. Gold(III) complexes tested as human AQP3 inhibitors.



Additional studies on other Au(III) compounds with different N<sup>N</sup> ligand scaffolds allowed us to establish preliminary structure-activity relationships.<sup>10</sup> Notably, Quantum Mechanics/Molecular Mechanics (QM/MM) calculations showed that the ligand moiety may play a major role in orienting the selectivity towards a certain isoform,<sup>10</sup> stabilizing the position of the inhibitor in the extracellular binding pocket

and possibly blocking the solutes' fluxes. Interestingly, Molecular Dynamics (MD) simulations on the adducts of  $\text{Hg}^{2+}$  ions (benchmark inhibitors of all AQPs<sup>11, 12</sup>) with AQP3 have allowed us to discover that pore closure may be due to protein conformational changes upon metal binding, other than direct steric blockage of the channel by the inhibitor.<sup>13</sup>

Following these promising results, we report here on the human AQP3 inhibition properties of four Au(III) complexes (Fig. 1), including three coordination complexes with a dipyrindin-2-ylamine (DipyAm) ligand  $[\text{Au}(\text{Dipyam})\text{Cl}_2]\text{PF}_6$  (**1**),<sup>14</sup> with (pyridyl)benzimidazole type ligands –  $[\text{Au}(\text{Pblm})\text{Cl}_2]$  (**3**) (Pblm = 2-(pyridin-2-yl)-benzimidazole)<sup>15</sup> and  $[\text{Au}(\text{PblmMe})\text{Cl}_2]\text{PF}_6$  (**4**) (PblmMe = 1-methyl-2-(pyridin-2-yl)-benzimidazole), respectively. Moreover, for the first time, an organometallic Au(III) compound with a C<sup>N</sup> cyclometalated 2-benzylpyridine ( $\text{py}^{\text{b-H}}$ ) ligand (**2**)<sup>16</sup> was tested as AQP inhibitor.

The mechanism of AQP3 inhibition by the most potent compound of the series was studied by MD simulations, allowing to disclose important structural changes leading to pore closure upon gold binding. Furthermore, the identification of structure-activity relationships that may link the electrochemical and electronic/structural properties of Au(III) compounds to their biological effects, was also explored. Thus, electrochemical methods were applied to define the compounds' electron-transfer abilities, while density functional theory (DFT) calculations were performed to further substantiate and interpret the experimental biological effects.

## Results and discussion

Compounds **1-3** were synthesized adapting previously reported procedures (see Experimental section). The new Au(III) complex **4** was obtained in 82% yield by reaction between 1-methyl-2-(pyridin-2-yl)-benzimidazole<sup>17</sup> in MeCN with an equimolar aqueous solution of  $\text{NaAuCl}_4$  and an excess of  $\text{PF}_6$  at room temperature (r.t.) for 3 h, and characterized by various methods. The gold complexes were tested for their AQP1 and AQP3 inhibition properties in hRBC by stopped-flow spectroscopy. The obtained results are summarized in Table S1 and Figure S1A in the Supplementary material. As previously observed for Auphen and related compounds,<sup>8, 10</sup> some of the new complexes act as inhibitors of glycerol permeation via AQP3, but do not affect water permeation via AQP1. The coordination complex **1** shows moderate inhibition of water and glycerol permeability ( $\text{IC}_{50} > 20 \mu\text{M}$ ), which may be due to its poor stability in physiological environment.<sup>14</sup> The organometallic compound  $[\text{Au}(\text{py}^{\text{b-H}})\text{Cl}_2]$  **2** was also scarcely active up to  $50 \mu\text{M}$ , maybe since the metal-carbon bond renders the Au(III) centre less prone to ligand exchange reactions. Interestingly, while the neutral complex **3** poorly inhibits glycerol transport ( $\text{IC}_{50} > 50 \mu\text{M}$ ), the novel cationic compound  $[\text{Au}(\text{PblmMe})\text{Cl}_2]\text{PF}_6$  **4** is a very potent AQP3 inhibitor ( $\text{IC}_{50} = 0.6 \pm 0.1 \mu\text{M}$ ), even more effective than Auphen, and ca. 3 orders of magnitude more potent than **3**. The reversibility of AQP3 inhibition was also studied pre-treating hRBC with the compounds for 30 min at r.t. and

subsequently washing the cells with either the thiol containing reducing agent *b*-mercaptoethanol (BME, 1 mM)<sup>18</sup> or with the sulfur donor L-Cys. In both cases, as shown in Figure S1B, both treatments with the competitor molecules led to an almost complete recovery of glycerol permeability, ruling out possible oxidative modification of amino acid residues by the Au(III) complex.

The mechanism of human AQP3 inhibition by complex **4** was analysed using classical molecular dynamics (MD). The quaternary structure of AQP3 was prepared via homology modelling, following an approach previously described by us<sup>13</sup> and described in the supplementary material. The compound was first parameterised using DFT and QM/MM to generate Au(III) parameters for the applied forcefield, and then directly bound to the thiolate of Cys40, in the form  $[\text{Au}(\text{PblmMe})\text{Cl}]^{2+}$ . Geometry optimisation was performed on this fragment (Fig. S2), which was subsequently embedded into monomer A of AQP3. The charge of Au was set to +3 (Au(III)). Afterwards, five independent MD simulations (0.5 ns) were conducted to determine the effect of **4** on water and glycerol permeation using either: i) AQP3 or ii) gold-bound AQP3 (AQP3-Au). Figure 2 shows the pore size comparison of the structures for monomer A obtained from two representative simulations. Complex **4** binding to Cys40 induces shrinkage of the pore, impeding both glycerol and  $\text{H}_2\text{O}$  permeability.

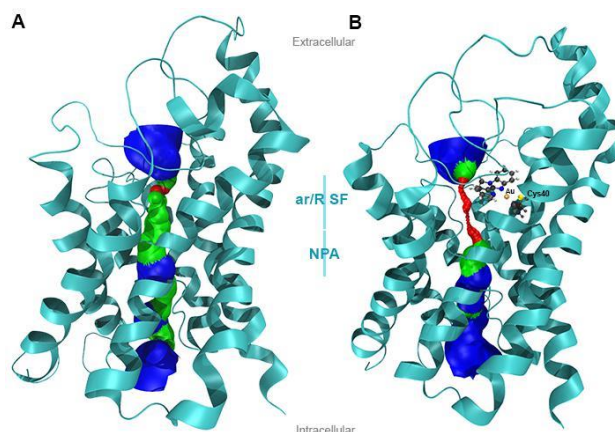


**Figure 2.** (A) Human AQP3 monomer A and (B) AQP3 with modified Cys40 (AQP3-4), showing the effect on pore size (based on VDW radii): red = smaller than single  $\text{H}_2\text{O}$ , green = single  $\text{H}_2\text{O}$ , blue = larger than single  $\text{H}_2\text{O}$ . Complex **4** and Cys40 are shown in ball and stick representation, with atoms coloured by atom type. Generated with HOLE<sup>20</sup> and VMD<sup>21</sup>.

From one simulation, 30 snapshots were taken and the pore size of each monomer measured as detailed in the supplementary material (Fig. S5). Afterwards, in order to validate the observed trend, five snapshots were taken (100, 300, 450, 600 and 800 frames) from each of the five independent simulations, and the pore size was measured in each. The average of size fluctuations was obtained (Fig. S6), and allowed to rule out spontaneous pore geometry fluctuations during the simulation. Remarkably, from the average of the pore size analysis, complex **4** binding to monomer A also constricts monomer D, although not sufficiently to hinder the solute permeability, but not B and C (Fig. S6).



The overall protein conformation is conserved upon gold binding, as shown by the root mean square displacement (RMSD) plots reported in Fig. S3. However, local conformational changes of both the protein surface (Fig. S7) and the pore lining can be observed. Specifically, binding of the complex induced rearrangement of the side chains of the aromatic/arginine selectivity filter (ar/R SF) (Fig. 3). Compound **4** does not appear to be positioned in the channel in a way that could prevent glycerol or water to flow through. However, binding of the complex, just above Arg218, prevents this residue from forming a H-bond with the backbone, present in the native AQP3, pushing the side-chain into the channel area (Fig. 3). These effects suggest that inhibition of AQP3's water and glycerol permeability is mainly due to protein conformational changes induced by binding of the gold complex to Cys40, rather than by the compound's steric hindrance, in line with the previous MD results on the binding of  $\text{Hg}^{2+}$  to AQP3.<sup>13</sup> It is worth mentioning that similar effects were observed when a longer MD simulation was run (8 ns, Fig. S8).

Moreover, the observed structural changes upon gold binding increase the hydrophobicity of the pore entrance of monomer A, due to increased exposure of hydrophobic side chains (Fig. S7). Overall, the symmetry of the tetramer is disrupted in the AQP3-Au model, as can be seen in Fig. S7, due to increased exposure of hydrophilic residues (e.g. Arg50 and Asp125). These relatively small changes appear to affect the approaching of glycerol molecules to the channels.

To further investigate why the two complexes **3** and **4** have different AQP3 inhibitory effects, and assuming Cys40 as the gold binding site as in the case of Auphen,<sup>9</sup> DFT calculations were performed on the adducts between a cysteinato ligand and compounds **2-4**, as well as Auphen, obtained by

substituting one of the two chlorido ligands (see Fig. S9). The energy values of adduct formation are reported in Table S2 and show that a larger formation energy is observed for positively charged Au(III) complexes with respect to neutral ones. These results support the hypothesis that the cationic compounds,  $[\text{Au}(\text{phen})\text{Cl}_2]^+$  and  $[\text{Au}(\text{PblmMe})\text{Cl}_2]^+$  **4** can be more easily complexed by cysteinato residues than the neutral complexes  $[\text{Au}(\text{py}^b)\text{Cl}_2]$  **2** and  $[\text{Au}(\text{Pblm})\text{Cl}_2]$  **3**. Therefore, the corresponding AQP3 inhibition effects perfectly match this trend.

Finally, we used cyclic voltammetry (CV) to evaluate the electrochemical features of the selected Au(III) complexes. Previous reports have investigated the electrochemistry of square planar Au(III) complexes with chlorido,<sup>22</sup> N^N donor<sup>23, 24</sup> and C^N^C donor<sup>25, 26</sup> ligands. Typical responses involve the reduction of Au(III) to Au(I) at potentials which are heavily influenced by the coordinating ligand field strength. Initially, we examined the electrochemical response of  $\text{HAuCl}_4$  in DMSO containing 0.1 M TBAP as a supporting electrolyte by CV (Fig. S10, in the Supplementary material). As expected, the introduction of strongly coordinating ligands, as in Auphen, shifts reduction potentials ( $\text{Au}^{\text{III/I}}$  reduction process) to more positive values.<sup>27</sup> Table S3 shows values of redox potentials

attributed to reductive ( $E_{\text{red}}$ ) and oxidative ( $E_{\text{ox}}$ ) electrochemical processes. Comparison of CVs of Auphen and

$\text{HAuCl}_4$  clearly shows this effect (Figure S11). Substitution of two chlorido ligands by a phen scaffold results in a shift of +0.33 V for the  $\text{Au}(\text{III}) \rightarrow \text{Au}(\text{I})$  process (Peak I vs. Peak I'). Similar voltammetric responses to Auphen were obtained for the complexes **2-4** (see Table S3) (see Fig. S12-14 in the Supp. material). As expected, **2** has the lowest reduction potential due to the C^N coordinating ligand.

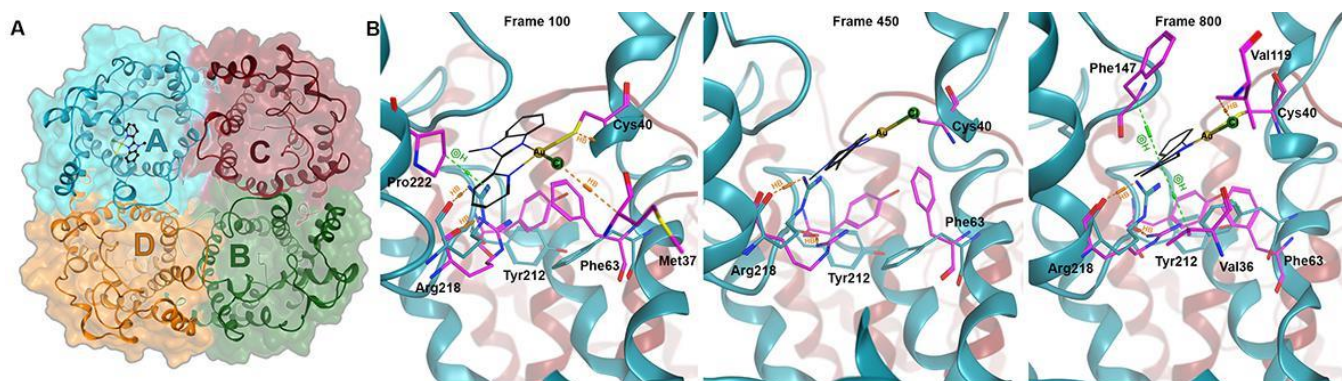


**Figure 3.** (A) Tetrameric view of human AQP3 bound to complex **4**. (B) Structure of the ar/R SF of AQP3 (blue) and upon binding of the gold complex (pink). The gold complex **4** is shown in black with thin sticks, gold in yellow-gold color and chloride in green, both in ball and stick representation. H-bonds are shown in orange dashed lines (HB), while H-arene interactions are shown in green dashed lines. Figures in panel B were generated with MOE.<sup>28</sup>

Moreover, potentials are shifted to more negative values with increasing electron donating character. For example, the Pblm ligand is more electron-donating than phen, so potentials are shifted by about -0.3 V.<sup>29</sup> Furthermore, the complexes yielded a second reduction peak (Peak II) indicative of  $\text{Au}(\text{I}) \rightarrow \text{Au}(\text{0})$  reduction process. Interestingly, all peak II potentials are centred at ca. -1.26 V, made exception for **2** (Table S3). Similar responses were reported for a range of Au(III) monodentate

pyridine complexes.<sup>30</sup> Interestingly, the organometallic complex **2** is predicted to form a C-Au-Cl complex after reduction. In fact, the voltammetric response of **2** differs from those of general formula  $\text{Au}(\text{N}^{\wedge}\text{N})\text{Cl}_2$ , with two successive reduction peaks at -0.99 V and -1.72 V. The main conclusion out of the CV studies is that the electrochemical properties of the Au(III) compounds do not directly correlate to their AQP3 inhibition effects, as, for example, complexes **3** and **4** have

similar redox potentials but markedly different effects on glycerol permeability.

## Conclusions

Due to the broad range of functions of AQPs in physiology and in disease states, the necessity of selective modulators (inhibitors) of AQPs is impellent, as these could be used as either chemical probes to detect their function in biological systems, or as innovative therapeutic agents in a variety of disease states. Here, a new series of Au(III) complexes has been studied for their AQP3 inhibition properties, and the cationic complex **4** was identified as the most potent inhibitor of glycerol permeation. Interestingly, the neutral complex **3**, with a similar ligand system, was scarcely active. DFT studies showed that a good correlation can be found between the compound's calculated affinity for cysteine residues and their AQP3 inhibitory activity. Instead, electrochemistry results suggest that the redox properties of the compounds do not influence their inhibition potency, therefore excluding AQP3 inhibition by oxidative damage.

Remarkably, MD studies conducted for the first time on the Au(III) complex binding to AQPs, have allowed to discover that protein conformational changes, upon metal binding to Cys40 in human AQP3, are mostly responsible for the observed inhibition of water and glycerol permeation. This finding has important implications for future inhibitors' design, in that other amino acid residues (even outside the channel) could be targeted, if their modification leads to the necessary conformational changes to achieve channel closure. Of note, the Au(III) complexes herewith described possess cytotoxic anticancer properties *in vitro*, and in recent years several gold compounds have shown promising anticancer effects related to the inhibition of different protein targets.<sup>31</sup> In this context, we cannot exclude that inhibition of AQP3 might also contribute to the biological effects of the reported compounds towards cancer cells, although other studies are ongoing in our labs to validate this hypothesis.

## Acknowledgements

Authors wish to acknowledge the help of Dr. A. Marrone and Ms. V. Graziani for help in defining the MM parameters for the gold complex. A.F. Mósca received a PhD fellowship (SFRH/BD/52384/2013) from Fundação para a Ciência e Tecnologia, Portugal.

## Notes and references

1. *Aquaporins in health and disease: new molecular targets for drug discovery*, CRC Press, Taylor & Francis Group, 2016.
2. G. Benga, *Mol Aspects Med*, 2012, **33**, 514-517.
3. A. de Almeida, G. Soveral and A. Casini, *MedChemComm*, 2014, **5**, 1444-1453.
4. A. S. Verkman, M. O. Anderson and M. C. Papadopoulos, *Nature Reviews Drug Discovery*, 2014, **13**, 259-277.
5. E. Beitz, A. Gollmack, M. Rothert and J. von Bulow, *Pharmacol Ther*, 2015, **155**, 22-35.
6. A. S. Verkman, *Annu Rev Med*, 2012, **63**, 303-316.
7. G. Soveral and A. Casini, *Expert Opin Ther Pat*, 2016, 1-14.
8. A. P. Martins, A. Marrone, A. Ciancetta, A. Galan Cobo, M. Echevarria, T. F. Moura, N. Re, A. Casini and G. Soveral, *PloS one*, 2012, **7**, e37435.
9. A. Serna, A. Galan-Cobo, C. Rodrigues, I. Sanchez-Gomar, J. J. Toledo-Aral, T. F. Moura, A. Casini, G. Soveral and M. Echevarria, *Journal of Cellular Physiology*, 2014, **229**, 1787-1801.
10. A. P. Martins, A. Ciancetta, A. de Almeida, A. Marrone, N. Re, G. Soveral and A. Casini, *ChemMedChem*, 2013, **8**, 1086-1092.
11. R. I. Macey and R. E. Farmer, *Biochimica et biophysica acta*, 1970, **211**, 104-106.
12. G. M. Preston, T. P. Carroll, W. B. Guggino and P. Agre, *Science*, 1992, **256**, 385-387.
13. A. Spinello, A. de Almeida, A. Casini and G. Barone, *J inorg. biochem.*, 2016, **160**, 78-84.
14. A. Casini, M. C. Diawara, R. Scopelliti, S. M. Zakeeruddin, M. Grätzel and P. J. Dyson, *Dalton transactions*, 2010, **39**, 2239-2245.
15. M. Serratrice, M. A. Cinellu, L. Maiore, M. Pilo, A. Zucca, C. Gabbiani, A. Guerri, I. Landini, S. Nobili, E. Mini and L. Messori, *Inorganic Chemistry*, 2012, **51**, 3161-3171.
16. M. A. Cinellu, A. Zucca, S. Stoccoro, G. Minghetti, M. Manassero and M. Sansoni, *Dalton Transactions*, 1996, 4217-4225.
17. W. K. Huang, C. W. Cheng, S. M. Chang, Y. P. Lee and E. W. Diau, *Chemical communications*, 2010, **46**, 8992-8994.
18. D. F. Savage and R. M. Stroud, *Journal of molecular biology*, 2007, **368**, 607-617.
19. J. P. Jambeck and A. P. Lyubartsev, *Journal of chemical theory and computation*, 2012, **8**, 2938-2948.
20. O. S. Smart, J. G. Neduvellil, X. Wang, B. A. Wallace and M. S. Sansom, *Journal of molecular graphics*, 1996, **14**, 354-360, 376.
21. W. Humphrey, A. Dalke and K. Schulten, *J. Molec. Graphics*, 1996, **14**, 33-38.
22. L. M. A. Monzon, F. Byrne and J. M. D. Coey, *Journal of Electroanalytical Chemistry*, 2011, **657**, 54-60.
23. L. Messori, F. Abbate, G. Marcon, P. Orioli, M. Fontani, E. Mini, T. Mazzei, S. Carotti, T. O'Connell and P. Zanella, *Journal of medicinal chemistry*, 2000, **43**, 3541-3548.
24. A. Corma, I. Domínguez, A. Doménech, V. Fornés, C. J. Gómez-García, T. Ródenas and M. J. Sabater, *Journal of Catalysis*, 2009, **265**, 238-244.
25. V. K. Au, W. H. Lam, W. T. Wong and V. W. Yam, *Inorganic chemistry*, 2012, **51**, 7537-7545.
26. T. Dann, D. A. Rosca, J. A. Wright, G. G. Wildgoose and M. Bochmann, *Chemical communications*, 2013, **49**, 10169-10171.
27. S. Zhu, W. Gorski, D. R. Powell and J. A. Walmsley, *Inorganic chemistry*, 2006, **45**, 2688-2694.
28. C. C. G. I. Molecular Operating Environment (MOE), 1010 Sherbooke St. West, Suite #910, Montreal, QC, Canada, H3A 2R7, 2017).
29. M. Serratrice, M. A. Cinellu, L. Maiore, M. Pilo, A. Zucca, C. Gabbiani, A. Guerri, I. Landini, S. Nobili, E. Mini and L. Messori, *Inorganic chemistry*, 2012, **51**, 3161-3171.
30. R. Corbo, T. P. Pell, B. D. Stringer, C. F. Hogan, D. J. Wilson, P. J. Barnard and J. L. Dutton, *JACS*, 2014, **136**, 12415-12421.
31. A. de Almeida, B. L. Oliveira, J. D. G. Correia, G. Soveral and A. Casini, *Coordination Chemistry Reviews*, 2013, **257**, 2689-2704.